ISSN 1392–1320 MATERIALS SCIENCE (MEDŽIAGOTYRA). Vol. 17, No. 4 2011

Spatial Inhomogeneity of Luminescence in III-Nitride Compounds

Gintautas TAMULAITIS*

Semiconductor Physics Department and Institute of Applied Research, Vilnius University, Sauletekio 9 – III, LT-10222 Vilnius, Lithuania

crossref http://dx.doi.org/10.5755/j01.ms.17.4.768

Received 14 September 2011; accepted 12 October 2011

The band gap of III-nitride semiconductors cover a wide range from 0.77 eV (band gap of InN) to 6.2 eV (AlN). Thus, light-emitting diodes emitting from infrared to deep into ultraviolet can be fabricated using ternary III-nitrides InGaN, AlGaN, and AlInN with appropriate composition. However, growing the compounds with any desirable composition often encounters substantial difficulties due to phase separation, structural quality of the epilayers, impurities and extended defects, etc. The spatial inhomogeneity of emission properties in III-nitride epilayers and quantum well structures provides an informative insight into carrier migration, localization, and recombination and is important for development of light-emitting devices. In this paper, we introduce the techniques for luminescence study with spatial resolution (microphotoluminescence, confocal microscopy, scanning near field optical microscopy and cathodoluminescence), discuss material properties leading to emission inhomogeneity and review results on spatial distribution of photoluminescence and cathodoluminescence in InGaN and AlGaN, which are the most important ternary III-nitride compounds for application in light-emitting devices.

Keywords: III-nitrides, InGaN, AlGaN, spatially-resolved luminescence, microphotoluminescence, confocal microscopy, scanning near field optical microscopy, cathodoluminescence.

1. INTRODUCTION

The high-brightness light-emitting diodes (LEDs) with worldwide market of up to $11 billion in 2011 became an important substitute for conventional lamps in many applications. A substantial breakthrough in LED applications came after the development of blue and white LEDs with active layers based on InGaN and GaN heterostructures. Introduction of aluminum into ternary AlGaN, InAlN or quaternary AlInGaN compounds enables growth of epilayers with wide band gaps of up to 6.2 eV corresponding to the band gap of AlN (see [1–3] for review), while increasing content of indium in InGaN shifts the band gap of this compound down to 0.77 eV, the band gap of binary InN (see [4] for review).

Though the lattice constant of the ternary compounds $A_xB_{1-x}N$, where A and B stands for In, Ga, and Al, linearly depends on the content x (Vegard's law), the composition dependence of the band gap is nonlinear and can be approximated by empirical expression

$$E_g^{ABN}(x) = (1-x)E_g^{BN} + xE_g^{AN} - bx(1-x), \quad (1)$$

where E_g denotes the band gap of the corresponding compound. At room temperature, 0.77 eV, 3.42 eV, and 6.13 eV are the band gaps of InN, GaN, and AlN, respectively. The bowing parameter b depends not only on compound composition but, possibly, also on strain, which strongly depends on substrate material, buffer layer used, growth conditions, layer thickness, etc. Thus, selection of the b value is ambiguous. For example, analysis of 20 references on b for AlGaN by Lee et al. [5], led to conclusion that b values can be grouped into four groups with b in the vicinity of quite different values of –0.8 eV, +0.53 eV, +1.3 eV, and +2.6 eV. Bowing parameters 2.4, 1, and 3.0 eV can be considered as typical for InGaN, AlGaN, and AlInN, respectively [1].

Whatever the value of b, the band gap of III-nitrides covers the entire range from infrared to deep UV, and LEDs emitting in this range can, in principle, be produced. However, growing of the compounds with any desirable composition often encounters substantial difficulties due to phase separation, structural quality of the epilayers, impurities and extended defects, etc. Moreover, even in the III-nitride epilayers and heterostructures without phase separation, a spatially inhomogeneous emission distribution is observed. The most obvious origin of the inhomogeneity is the band gap modulation due to fluctuations in compound composition. For example, locally higher indium content in InGaN crystal results in a narrower band gap in this location. Other mechanisms can also be responsible for potential fluctuations and are discussed shortly in this review.

The most straightforward approach for study of the spatial emission inhomogeneity is application of photoluminescence (PL) or cathodoluminescence (CL) spectroscopy techniques enabling spatial resolution. These techniques will be introduced before discussion of the results obtained in InGaN and AlGaN epilayers and heterostructures.

2. TECHNIQUES FOR SPATIALLY-RESOLVED LUMINESCENCE SPECTROSCOPY

The simplest and least expensive technique for achieving spatial resolution in luminescence spectroscopy

*Corresponding author. Tel.: +370-5-2366071, fax.: +370-5-2366070. E-mail address: *gintautas.tamulaitis@ff.vu.lt* (G.Tamulaitis)

is micro-photoluminescence (μ-PL). The excitation light is focused as tightly as possible, and the luminescence is collected from the excited spot. The spatial resolution in this approach is, first of all, limited by aberrations of the optical systems used. The aberrations can be diminished or compensated by using appropriate design and materials for the optical systems. Nevertheless, the minimal spot size is limited by self-diffraction even for ideal optical systems. According to the Rayleigh criterion, the minimal spot size for a planar wavefront

$$d_R = 0.61\lambda/NA\,, \tag{2}$$

where $NA = n\cdot\sin\theta$ is the numerical aperture, n is the refraction index, θ is the half angle between the marginal converging rays of the light cone. For modern microscope objectives, NA values of up to ~1 can be achieved. Application of immersion liquids increases NA by n: 1.33 for water, 1.56 for oil. Thus, the self-diffraction limit of the spatial resolution obtainable with high-quality objectives equals approximately half the wavelength of the light used. A typical spatial resolution in real μ-PL systems equals ~1 μm.

A higher spatial resolution can be achieved in scanning confocal microscopes (SCMs) [6 – 8]. The configuration of the confocal microscope is depicted in Fig. 1. The same objective is used both for focusing the excitation light and for collecting the luminescence. The image plane of the collection system coincides with a screen containing a tiny aperture directly on the optical axis of the system. Thus, only the light coming out from a small spot on the sample surface passes the aperture and is detected directly by a detector or is analyzed by a spectrometer. The lateral resolution can be approximated as

$$d_{xy} \approx 0.4\lambda/NA\,. \tag{3}$$

A typical value for the lateral spatial resolution of conventional SCMs in the green region is ~200 nm. The surface of the sample under study can be scanned by moving the piezoelectric stage with the sample.

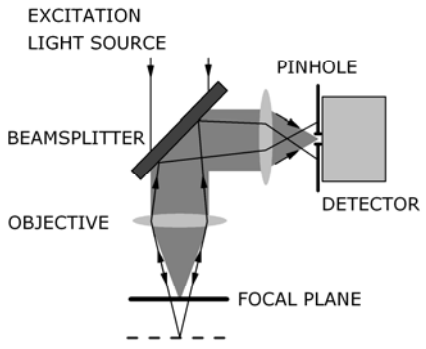

Fig. 1. Configuration of confocal microscope

Another advantage of SCMs is their capability of on-axis spatial resolution. As shown in Fig. 1, only the light emitted from the sample surface is focused into the aperture, while the light coming from the deeper parts of the sample forms a large, blurred-out image, and only a small part of it passes the aperture. However, the focal plane can be shifted deeper into the sample by moving the objective. Thus, a spatial resolution along the z-axis can be achieved. The resolution depends on the effective wavelength λ, which is related to the wavelengths of excitation (λ_{exc}) and luminescence (λ_{lum}) as $1/\lambda = 1/\lambda_{exc} + 1/\lambda_{lum}$, and can be approximated as

$$d_z \approx 1.4\lambda n\,/NA^2\,. \tag{4}$$

For λ = 0.5 μm and typical objective (NA = 0.9) in air (n = 1), the d_z value equals 0.86 μm.

The axial spatial resolution can be increased by the factor of up to five by using a group of techniques called 4-Pi confocal. Interference of two excitation light beams is utilized in the 4-Pi confocal microscope.

Self-diffraction limits the spatial resolution of optical systems only in the far field, i. e., when the distance from the light source considerably exceeds the wavelength. The limit can be substantially decreased in the near field when applying the technique that is called either Scanning Near-Field Optical Microscopy (SNOM) or Near-Field Scanning Optical Microscopy (NSOM). An aperture with the diameter smaller than the wavelength blocks the light in the far field but the light extends outside such an aperture in the near field, approximately to the distance equal to the aperture diameter $d << \lambda$. As illustrated in Fig. 2, making the aperture on the apex of a narrow tip enables scanning the sample surface with a high spatial resolution considerably exceeding the wavelength. Tapered metal-coated fused-silica single-mode optical fibers or hollow silicon cone tips are currently used in SNOM.

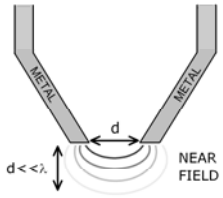

Fig. 2. Field distribution near the tip of a scanning near-field optical microscope (SNOM)

Spatial resolution in the devices containing apertures is basically determined by the aperture diameter. However, the throughput of the probe decreases as the sixth power of the aperture diameter. Thus, a trade-off between the spatial resolution and the intensity of luminescence available for detection has to be considered in planning experiments. Resolution reaching $\lambda/40$ is demonstrated [9] but majority of the SNOM systems currently in use exploit apertures enabling resolution of ~100 nm ($\sim\lambda/5$). A good spatial resolution can be achieved in apertureless configuration devices, where a sharp metal tip is used as a probe. Due to electron oscillations in the probe tip excited by illumination in the far field, the light field directly below the tip is enhanced by many orders of magnitude, and the sample is effectively excited only there. Unfortunately, the background luminescence detected from the area outside the tip might be substantial and impede the detection of the desirable signal from beneath the tip.

The surface is usually scanned by moving the sample mounted on a piezoelectric sample stage. The tip in SNOM devices is maintained at a fixed distance above the sample surface by using the same feedback systems as those used in atomic force microscopy (AFM), which is a more mature measurement technique.

SNOM devices can be configured in different modes. In illumination (I) mode, the sample is excited through the probe in the near field, and the luminescence is detected in the far field, thus the emission is detected from the entire excited area that can exceed the excitation spot due to diffusion or other spreading mechanisms. In collection (C) mode, the sample surface is homogeneously excited in the far field, while the spatial distribution of the luminescence is probed by collecting the light through the probe in the near field. In illumination-collection (I-C) mode, both excitation and detection are accomplished through the probe.

Short pulse laser excitation and luminescence detection in time-resolved mode by exploiting streak camera are also used in SNOM devices [10]. A dual-probe SNOM system independently controlling the distances between probe and sample and between two probes provides additional information, as demonstrated in real time study of carrier diffusion in InGaN [11].

High spatial resolution and capability of simultaneous measurement of PL distribution and surface morphology can be pointed out as the main advantages of SNOM technique. However, SNOM did not become a routine technique is spectroscopy due to several difficulties. In addition to the small signal to be detected, since the excitation volume or/and the probed volume are small, comparability of the experimental results is a considerable problem in SNOM applications due to deviations in aperture diameters of different tips, roughness of the aperture edges or the metallic coating of the tip, and possible wearing of the tip during experiment.

According to equation (1), the excitation spot size can be diminished by using excitation with a shorter wavelength. In cathodoluminescence (CL), using excitation by electrons with energy E corresponding to the wavelength $\lambda = hc/E$, which is substantially shorter than that of the light, enables a considerable gain in the spatial resolution. The spatial resolution in CL experiments can reach 1 nm and is usually restricted by instrumental limitations rather than by physical limits. Electrons in CL experiments are usually provided by electron gun and have energies of 0.1 keV – 30 keV. The electron beam creates backscattered electrons, secondary electrons, Auger electrons, X-rays and photons in visible, UV, or IR ranges. Thus, interpretation of the CL results is sometimes more complicated but informative. The CL experiments are usually carried out in either a scanning electron microscope (SEM) or a scanning transmission electron microscope (TEM). Matching CL results with structural characterization using SEM or TEM is a considerable advantage of CL technique. CL spectroscopy can also be accomplished in time-resolved mode. Fast deflecting of the electron beam away from the spot under study using deflection plates or an optically driven electron gun [12] are used to accomplish the time resolution. The latter technique ensures a better time resolution up to subpicosecond domain.

3. ORIGIN OF INHOMOGENEOUS SPATIAL DISTRIBUTION OF LIGHT EMISSION IN III-NITRIDE EPILAYERS AND HETEROSTRUCTURES

III-nitride epilayers exhibit inhomogeneous spatial distribution of luminescence properties. There are several origins for this inhomogeneity. First of all, most of III-nitride epilayers are grown on foreign substrates. Sapphire currently dominates as substrate material but SiC, Si, and other monocrystals are also used, though at a considerably lower extend [13]. Bulk GaN [14, 15] and AlN [16] substrates are being developed but their size is still small and their price is still high. Recently, hydride vapor phase epitaxy (HVPE) is proved to be prospective for growing thick, bulk-like GaN [17, 18] and AlN [19] layers that can be removed from the sapphire substrate by laser lift-off and used as free-standing substrates for homoepitaxy of these materials.

Most of III-nitride layers are grown by metal-organic chemical vapor deposition (MOCVD) using heteroepitaxy on sapphire. Low-temperature-grown buffer layers are usually deposited to accommodate the lattice mismatch and to facilitate growing of the subsequent layers of better structural quality. The growth of the buffer layer starts by formation of nucleation islands that gradually coalesce. Temperature and V/III precursor ratio serve as the main parameters influencing formation of the buffer layer. For example, a lower V/III ratio enhances 3D growth mode and surface mobility, though increases the roughness of the layer [20]. The larger are the islands, the smaller are the areas of coalescence, where formation of structural defects, especially dislocations, has a higher probability. The dislocation density in the coalescence regions of the buffer layer is higher, and most of these dislocations extend to subsequent layers deposited on the buffer. Very high dislocation density is one of the major problems in growing III-nitride epilayers and heterostructures. Various more sophisticated buffer layers, including epitaxial lateral overgrowth (ELOG) [21] and ELOG variations using patterned substrates, have been developed. However, spatial inhomogeneity in the structure of the buffer layer might often be the origin of luminescence inhomogeneity in the layers deposited above the buffer.

Another origin of the PL spatial inhomogeneity in ternary or quaternary III-nitrides is composition fluctuations in access of local statistical fluctuations expected in a random alloy. Since the variations in composition results in local variations in the band gap, they can cause carrier (exciton) localization in small-scale potential minima and their accumulation in extended regions, where the average potential is lower. Large indium content in InGaN might also lead to phase separation of the compound. Thermodynamic calculations showed that there is a miscibility gap in the InGaN system and that for a typical growth temperature of 600 °C the alloy decomposes into In-rich and In-poor regions at In content exceeding just 6 % [22]. Strain shifts the

decomposition limit to considerably higher indium contents and the phase separation also depends on the growth conditions. Nevertheless, difficulties in avoiding the phase separation in high indium content InGaN strongly inhibits fabrication of InGaN-based LEDs emitting in green, yellow and red regions. No phase separation was theoretically predicted for AlGaN compound [23]. However, this compound also exhibits carrier localization effects.

The inhomogeneous distribution of indium atoms should cause an inhomogeneous strain. III-nitride semiconductors are piezoelectric. Thus, strain occurring at a heterointerface causes an electric field. Electric field also occurs due to different polarity of the adjacent materials. The built-in field due to both piezoelectric and spontaneous polarization in quantum wells results in the quantum-confined Stark effect: the field transforms the quantum well from rectangular to triangular shape, the emission band shifts to long-wavelength side, and the probability of radiative recombination decreases, since the overlap of electron and hole wavefunctions decreases due to spatial separation of the recombining electron and hole in the triangular quantum well. The built-in electric field can be calculated using material parameters [24]. However, interpretation of certain experimental results in AlGaN heterostructures requires smaller field values than those calculated using material parameters available to date [25, 26]. Anyway, spatial inhomogeneity in strain might result in inhomogeneity in PL properties. At high density of nonequilibrium carriers, the built-in field might be screened. The screening effect can be taken into account theoretically by simultaneously solving the stationary Schrödinger equation and the Poisson equation.

The localized regions of strain contrast [27, 28] and lattice fringe displacement [29, 30] observed in high resolution transmission electron microscopy (HR-TEM) have been attributed to the inhomogeneous composition in InGaN compound. However, the further TEM study showed that the strain inhomogeneities might be introduced in the material due to electron beam damage [31].

The effective band gap of quantum wells might have substantial spatial variations due to well width fluctuations. For narrow QWs with widths of the order of several nanometers (typical for LED and laser diode structures), even fluctuations of the well width by one monolayer result in variation in the effective band gap by tens of meV. Thus, the areas with broader QWs serve for carrier localization or accumulation.

Inhomogeneous strain at the interfaces might also cause potential fluctuations leading to inhomogeneous PL distribution.

According to theoretical calculations, carriers might be localized even in homogeneous InGaN due to localization of the hole wave functions around In along randomly formed In-N-In chains [32, 33]. There are no corresponding calculations in hexagonal InGaN, which is the usual modification of InGaN, but the recent results on positron annihilation are in consistence with the model of localization on such In-N-In chains in hexagonal InGaN [34].

4. SPATIAL DISTRIBUTION OF LIGHT EMISSION IN InGaN EPILAYERS AND HETEROSTRUCTURES

Though InGaN is currently the material of choice for active media in blue and white LEDs and blue laser diodes, peculiarities of carrier (exciton) localization in this compound are still not fully understood. It is generally accepted that nonequilibrium carriers in ternary InGaN compounds are localized in potential fluctuations occurring due to inhomogeneous distribution of indium in epilayers or/and due to variation in the well width in multiple quantum well (MQW) structures. The spatial scale of these fluctuations is still a matter of discussions and might range in different samples from micrometers [35] down to interatomic distances. In-plane localization on the length scale of approximately 2 nm was observed in InGaN/GaN QWs by analyzing the intensity ratio between the zero-phonon low-temperature PL bands and their phonon replicas to estimate the Huang-Rhys factor. The dependence of the Huang-Rhys factor on electron-hole separation was utilized. The separation depends on the piezoelectric field due to strain at the QW interfaces, while the piezoelectric effect depends on indium content in the GaN/InGaN/GaN heterostructure [36]. Sharp lines emerging in low-temperature PL spectra of InGaN mesas, when the mesa size is diminished down to submicrometer range, are also considered as an evidence of emission by localized excitons [37]. On the other hand, no evidence on deviations of indium distribution from that expected in a random alloy was found using three-dimensional atom probe analysis [38].

Probable, different InGaN epilayers and QWs, especially those with different indium content, have the potential profile fluctuations with considerable variations in their depth and spatial extent.

The carrier localization usually causes an abnormal temperature dependence of PL band peak position and width. In semiconductors without localization, the temperature dependence of the PL band peak follows the continuous band gap shrinkage phenomenologically described by the Varshni formula [39] or a Bose-Einstein-like formula [40]. In semiconductors with considerable carrier localization, the temperature dependence of the PL band peak position has an S-shape. The PL band initially redshifts due to the thermally enhanced ability of localized excitons to reach the lowest available energy sites via hopping [41 – 43]. The further increase in temperature facilitates thermalization of the exciton system, causes a high-energy shift of the exciton distribution and, consequently, a blue shift of the PL band [41]. Finally, the temperature-induced band gap shrinkage starts to dominate and shifts the emission band to longer wavelengths again. Simultaneously, the band width experiences a W-shaped temperature dependence.

Based on comparison of the experimentally observed temperature dependences of PL band characteristics with results obtained using Monte Carlo simulation of exciton hopping, a double-scale potential fluctuation model has been suggested: excitons in InGaN accumulate in areas with higher indium content and experience random

potential fluctuations at a smaller spatial scale when moving within these areas [44].

Bright spots of the order of hundreds of nanometers in diameter on the background with lower emission intensity have been observed more than a decade ago in CL images of InGaN single quantum wells (see Fig. 3) and were interpreted by existance of quantum discs due to compositional undulations in the quantum well [45].

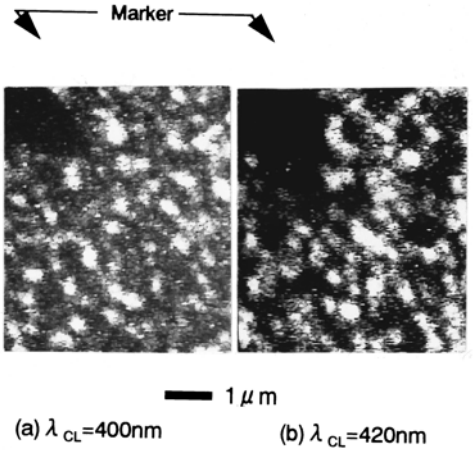

Fig. 3. Monochromated CL images of $In_{0.2}Ga_{0.8}N$ single quantum well at wavelengths of 400 nm (a) and 420 nm (b). Reproduced from [45] with permission

As discussed above, early results on transmission electron microscopy (TEM) have been interpreted as a direct evidence of the inhomogeneous In distribution in InGaN epilayers. However, the further TEM study demonstrated that the In-rich "clusters" observed might be created by the electron beam used in TEM characterization [31, 46]. Nevertheless, cathodoluminescence [45, 47 – 49], μ-PL [50 – 52], confocal spectroscopy [53 – 55], and scanning near field optical microscopy (SNOM) [56 – 59] reveal inhomogeneous photoluminescence intensity distribution in InGaN epilayers and QWs.

Well width fluctuations are pointed out as the main origin of exciton localization in InGaN QWs in many publications [60, 36, 61]. Correlation between well width variations and emission intensity has been demonstrated by comparison of atomic force microscopy and CL images [62].

Usually, the PL bands in the bright areas of InGaN epilayers and MQWs are redshifted in respect of their positions in the dark areas. This is in consistence with the model assuming that the carriers tend to accumulate in the areas with a lower potential. Thus, the photons emitted in these regions have, in average, lower energies than those emitted in the dark areas. Nevertheless, an oposite correlation between PL intensity and band position is also observed in certain InGaN structures [63, 59]. The correlations of three types were observed in violet, blue, and green-emitting SQWs (see Fig. 4). Comparison of the results obtained by using SNOM in I-C and I modes led to conclusion that the different correlations are caused by indium-content-dependent carrier localization conditions that influence capability of the carriers to reach nonradiative recombination centers [59].

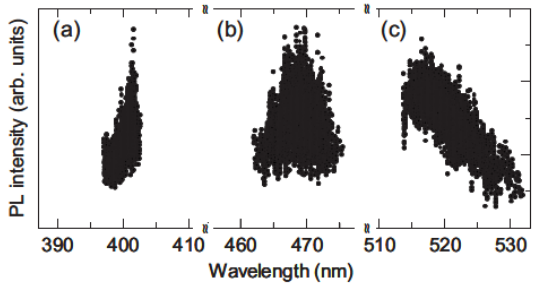

Fig. 4. Relationship between peak intensity and wavelength of PL probed by SNOM in the *I–C* mode in $In_xGa_{1-x}N$ SQWs emitting in violet (a), blue (b), and green (c) regions. Reproduced from [59] with permission

The red shift of PL band in dark areas in respect to its position in the bright areas observed in InGaN-based LED structures were shown to occur as a result of predominant nonradiative recombination of less localized carriers (excitons), which are responsible for short-wavelength side of PL band (see Fig. 5). This effect is more pronounced in areas with a higher defect density. Thus, it was shown that the inhomogeneous defect density might be responsible for inhomogeneous PL distribution [63].

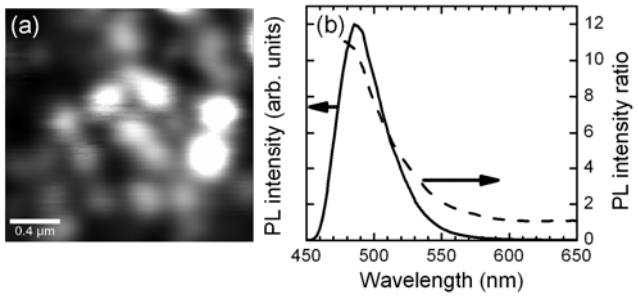

Fig. 5. PL intensity mapping (2 μm × 2 μm) image of InGaN-based LED structure (a) and spatially-integrated PL spectrum in bright areas (solid curve) and spectral distribution of ratio of PL intensity spatially integrated in bright and dark areas (dashed curve) (b). After [63]

Inhomogeneous carrier distribution in the well plane might also be influenced by threading dislocations. Hexagonal V-shaped pits formed around the threading dislocations under appropriate conditions exhibit narrow sidewall quantum wells with an effective band gap significantly larger than that of the regular quantum well [64]. SNOM spectroscopy in combination with TEM study has been successfully used to reveal "antilocalizing" potential barriers around such dislocations and to clearly elucidate an important mechanism preventing nonradiative carrier recombination at dislocations in InGaN MQWs [64] (see Fig. 6). The quantum wells on the side walls of the V-shaped pit in the vicinity of a threading dislocation crossing the InGaN MQW structure are narrower than those in the areas free of dislocations. Accordingly, high and low energy bands appear in the PL spectra recorded by using SNOM (see Fig. 6, c). Formation of the region with a higher potential due to the narrower quantum well prevents the carriers from reaching the dislocation and recombining nonradiatively there.

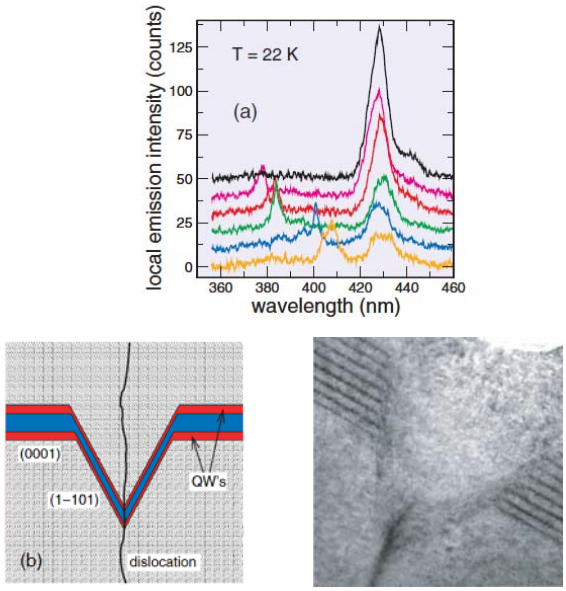

Fig. 6. PL spectra obtained using SNOM in the vicinity of threading dislocation (a), sketch (b) and transmission electron microscope image (c) of V-shaped pit around dislocation crossing InGaN/GaN MQW structure. Reproduced from [64] with permission

5. SPATIAL DISTRIBUTION OF LIGHT EMISSION IN AlGaN STRUCTURES

The S-shaped temperature dependence of PL band position that, as discussed above, is an indication of carrier localization was observed in AlGaN epilayers together with other evidences showing that alloy clustering is quite possible in this compound [65 – 68]. A double-scaled potential profile has been elucidated by comparing experimental results with Monte Carlo simulation of exciton hopping and recombination [68]. It was also shown that the density of nonradiative recombination centers is a key issue in achieving a better LED performance, since a considerable difference in carrier lifetimes was observed in $Al_{0.26}Ga_{0.74}N$ epilayers with very similar potential profiles.

Spatially nonuniform intensity distribution of redshifted emission was observed in CL images at room-temperature in AlGaN samples grown by plasma-assisted molecular-beam epitaxy with 20 % – 50 % of aluminum [69]. The emission inhomogeneities were attributed to compositional inhomogeneity. The results obtained using time-resolved CL spectroscopy of $Al_xGa_{1-x}N$ epilayers with $0.05 < x < 0.25$ were consistent with the potential fluctuation model. At low temperatures, when the excitons are strongly localized, the exciton lifetime increases monotonically with aluminum content, while at elevated temperatures the excitons are delocalized, the decay becomes faster and predominantly nonradiative, regardless of the aluminum content.

There are only a couple of papers reporting on SNOM study of AlGaN [70, 71].

Using SNOM in I-C mode, a dual localization pattern in AlGaN epilayers with the AlN molar fraction varying from 0.30 to 0.50 was elucidated [71]. The potential fluctuations on 100 nm spatial scale were evaluated from the width of the photoluminescence spectra. The fluctuation depth varied between 0 meV and 51 meV and increased with increased Al content. These potential variations have been assigned to small-scale compositional fluctuations due to stress variations, dislocations, and existance of Al-rich grains. The larger area potential variations of 25 meV – 40 meV in depth were especially pronounced in the low Al-content epilayers and have been attributed to Ga-rich regions close to grain boundaries or atomic layer steps. Maps of localization parameter σ_L and sketches of potential profiles in AlGaN epilayers containing different molar fraction of aluminum are presented in Fig. 7.

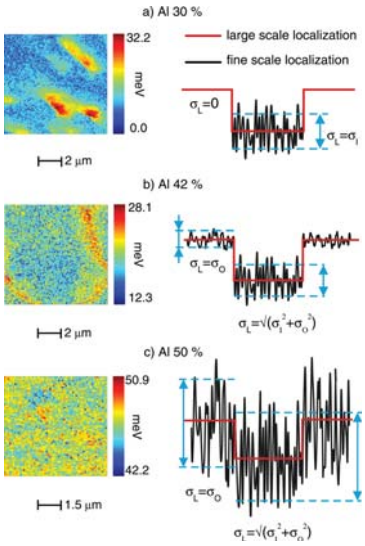

Fig. 7. Maps of localization parameter σ_L for AlGaN epilayers with different Al content (indicated) and sketches of potential profiles in the corresponding epilayers. Reproduced from [71] with permission

SNOM study of low-Al-content AlGaN epilayers and quantum wells with different well widths revealed correlation between the PL intensity and band peak wavelength. This correlation was attributed to inhomogeneous screening of the built-in electric field [70].

6. CONCLUSIONS

Spatial inhomogeneity of radiative and nonradiative recombination of nonequilibrium carriers in III-nitride epilayers and heterostructures reflect complicated composition fluctuations, inhomogeneous point defect distribution, influence of dislocations, strain variations. Better understanding of these properties and processes is desirable for purposeful development of light emitting devices, sensors and transistors based on this prospective semiconductor family. Techniques for luminescence study with spatial resolution down to subwavelength range are powerful tools to study the spatially inhomogeneous emission properties. Combination of these techniques with conventional luminescence spectroscopy and structural analysis provided a considerable contribution in study of III-nitrides and have good prospects for further applications.

Acknowledgments

The article was prepared under support of the European Social Fund Agency implementing measure VP1-3.1-ŠMM-05-K of the Human Resources Development Operational Programme of Lithuania 2007-2013 3rd priority "Strengthening of capacities of researchers and scientists" (project No. VP1-3.1-ŠMM-05-K-01-003)

REFERENCES

1. **Shur, M. S., Gaska, R.** Deep-Ultraviolet Light-Emitting Diodes *IEEE Transactions on Electron Devices* 57 2010: pp. 12 – 25. http://dx.doi.org/10.1109/TED.2009.2033768
2. **Khan, A., Balakrishnan, K., Katona, T.** *Nature Photonics* 2 2008: pp. 77 – 84. http://dx.doi.org/10.1038/nphoton.2007.293
3. **Khan, A., Shatalov, M., Maruska, H. P., Wang, H. M., Kuokstis, E.** III-Nitride UV Devices *Japanese Journal of Applied Physics* 44 2005: pp. 7191 – 7206. http://dx.doi.org/10.1143/JJAP.44.7191
4. **Wu, J.** When Group-III Nitrides Go Infrared: New Properties and Perspectives *Journal of Applied Physics* 106 2009: p. 011101.
5. **Lee, S. R., Wright, A. F., Crawford, M. H., Petersen, G. A., Han, J., Biefeld, R. M.** The Band-gap Bowing of $Al_xGa_{1-x}N$ Alloys *Applied Physics Letters* 74 1999: pp. 3344 – 3346. http://dx.doi.org/10.1063/1.123339
6. **Pawley, J. B.** Handbook of Biological Confocal Microscopy. 1995: p. 2.
7. **Corle, T. R., Kino, G. S.** Confocal Scanning Optical Microscopy and Related Imaging Systems. 1996: p. 39.
8. **Murphy, D. B.** Fundamentals of Light Microscopy and Electronic Imaging. 2001.
9. **Betzig, E., Trautman, J. K., Harris, T. D., Weiner, J. S., Kostelak, R. L.** Breaking the Diffraction Barrier – Optical Microscopy on a Nanometric Scale *Science* 251 1991: p. 1468.
10. **Kaneta, A., Okamoto, K., Kawakami, Y., Fujita, Sh., Marutsuki, G., Narukawa, Y., Mukai, T.** Spatial and Temporal Luminescence Dynamics in an $In_xGa_{1-x}N$ Single Quantum Well Probed by Near-field Optical Microscopy *Applied Physics Letters* 81 2002: p. 4353.
11. **Kaneta, A., Hashimoto, T., Nishimura, K., Funato, M., Kawakami, Y.** Visualization of the Local Carrier Dynamics in an InGaN Quantum Well Using Dual-Probe Scanning Near-Field Optical Microscopy *Applied Physics Express* 3 2010: p. 102102.
12. **Merano, M., Sonderegger, S., Crottini, A., Collin, S., Renucci, P., Pelucchi, E., Malko, A., Baier, M. H., Kapon, E., Deveaud, B., Ganie`re, J.-D.** Probing Carrier Dynamics in Nanostructures by Picosecond Cathodoluminescence *Nature* 438 2005: pp. 479 – 482.
13. **Liu, L., Edgar, J. H.** Substrates for Gallium Nitride Epitaxy *Materials Science and Engineering R* 37 2002: p. 61. http://dx.doi.org/10.1016/S0927-796X(02)00008-6
14. **Porowski, S.** Bulk and Homoepitaxial GaN-growth and Characterisation *Journal of Crystal Growth* 189 1998: pp. 153 – 158.
15. **Dwilinski, R., Doradzinski, R., Garczynski, J., Sierzputowski, L. P., Puchalski, A., Kanbara, Y., Yagi, K., Minakuchi, H., Hayashi, H.** Excellent Crystallinity of Truly Bulk Ammonothermal GaN *Journal of Crystal Growth* 310 2008: p. 3911. http://dx.doi.org/10.1016/j.jcrysgro.2008.06.036
16. **Grandusky, J. R., Gibb, S. R., Mendrick, M. C., Moe, C., Wraback, M., Schowalter, L. J.** High Output Power from 260 nm Pseudomorphic Ultraviolet Light-Emitting Diodes with Improved Thermal Performance *Applied Physics Express* 4 2011: p. 082101.
17. **Usui, A., Sunakawa, H., Sakai, A., Yamaguchi, A. A.** Thick GaN Epitaxial Growth with Low Dislocation Density by Hydride Vapor Phase Epitaxy *Japanese Journal of Applied Physics* 36 1997: pp. L899 – L902.
18. **Monemar, B., Larsson, H., Hemmingsson, C., Ivanov, I. G., Gogova, D.** Growth of Thick GaN Layers with Hydride Vapour Phase Epitaxy *Journal of Crystal Growth* 281 2005: pp. 17 – 31.
19. **Kumagai, Y., Yamane, T., Koukitu, A.** Growth of Thick AlN Layers by Hydride Vapor-phase Epitaxy *Journal of Crystal Growth* 281 2005: pp. 62 – 67.
20. **Kim, S., Oh, J., Kang, J., Kim, D., Won, J., Kim, J. W., Cho, H.-K.** Two-step Grrowth of High Quality GaN Using V/III Ratio Variation in the Initial Growth Stage *Journal Crystal Growth* 262 2004: pp. 7 – 13.
21. **Kapolnek, D., Keller, S., Vetury, R., Underwood, R. D., Kozodoy, P., Baars, S. P. D., Mishra, U. K.** Anisotropic Epitaxial Lateral Growth in GaN Selective Area Epitaxy *Applied Physics Letters* 71 1997: pp. 1204 – 1206. http://dx.doi.org/10.1063/1.119626
22. **Ho, I., Stringfellow, G. B.** Solid Phase Immiscibility in GaInN *Applied Physics Letters* 69 1996: p. 2701. http://dx.doi.org/10.1063/1.117683
23. **Matsuoka, T.** Phase Separation in Wurtzite $In_{1-x-y}Ga_xAl_yN$ *Journal of Nitride Semiconductors Research* 3 1998: p. 54.
24. **Bernardini, F., Fiorentini, V.** Macroscopic Polarization and Band Ofsets at Nitride Heterojunctions *Physics Review B* 57 1998: p. R9427.
25. **Pinos, A., Marcinkevičius, S., Liu, K., Shur, M. S., Kuokštis, E., Tamulaitis, G., Gaska, R., Yang, J., Sun, W.** Screening Dynamics of Intrinsic Electric Field in AlGaN Quantum Wells *Applied Physics Letters* 92 2008: p. 061907. http://dx.doi.org/10.1063/1.2857467
26. **Mickevičius, J., Kuokštis, E., Liuolia, V., Tamulaitis, G., Shur, M. S., Yang, J., Gaska, R.** Photoluminescence Dynamics of AlGaN Quantum Wells with Built-in Electric Fields and Localized States *Physica Status Solidi A* 207 2010: p. 423.
27. **Lin, Y.-S., Ma, K.-J., Hsu, C., Feng, S.-W., Cheng, Y.-C., Liao, C.-C., Yang, C. C., Chou, C.-C., Lee, C.-M., Chyi, J.-I.** Dependence of Composition Fluctuation on Indium Content in InGaN/GaN Multiple Quantum Wells *Applied Physics Letters* 77 2000: p. 2988. http://dx.doi.org/10.1063/1.1323542
28. **Cho, H. K., Lee, J. Y., Sharma, N., Humphreys, C. J., Yang, G. M., Kim, C. S., Song, J. H., Yu, P. W.** Effect of Growth Interruptions on the Light Emission and Indium Clustering of InGaN/GaN Multiple Quantum Wells *Applied Physics Letters* 79 2001: p. 2594. http://dx.doi.org/10.1063/1.1410362
29. **Gerthsen, D., Hahn, E., Neubauer, B., Rosenauer, A., Schön, O., Heuken, M., Rizzi, A.** Composition Fluctuations in InGaN Analyzed by Transmission Electron Microscopy *Physica Status Solidi A* 177 2000: p. 145.
30. **Ruterana, P., Kret, S., Vivet, A., Maciejewski, G., Dluzewski, P.** Composition Fluctuation in InGaN Quantum Wells Made from Molecular Beam or Metalorganic Vapor Phase Epitaxial Layers *Journal of Applied Physics* 91 2002: p. 8979.

31. **Smeeton, T. M., Kappers, M. J., Barnard, J. S., Vickers, M. E., Humphreys, C. J.** Electron-Beam-Induced Strain within InGaN Quantum Wells: False Indium "Cluster" Detection in the Transmission Electron Microscope *Applied Physics Letters* 83 2003: pp. 5419 – 5421.
32. **Bellaiche, L., Mattila, T., Wang, L.-W., Wei, S. H., Zunger, A.** Resonant Hole Localization and Anomalous Optical Bowing in InGaN Alloys *Applied Physics Letters* 74 1999: p. 1842. http://dx.doi.org/10.1063/1.123687
33. **Kent, P. R. C., Zunger, A.** Carrier Localization and the Origin of Luminescence in Cubic InGaN Alloys *Applied Physics Letters* 79 2001: pp. 1977 – 1979. http://dx.doi.org/10.1063/1.1405003
34. **Chichibu, S. F., Takeyoshi, A. U., Onuma, A., Haskell, B. A., Chakraborty, A., Koyama, T., Fini, P. T., Keller, S., Denbaars, S. P., Speck, J. S., Mishra, U. K., Nakamura, S., Yamaguchi, S., Kamiyama, S., Amano, H., Akasaki, I., Han, J., Sota, T.** Origin of Defect-insensitive Emission Probability in In-containing (Al,In,Ga)N Alloy Semiconductors *Nature Materials* 5 2006: pp. 810 – 816. http://dx.doi.org/10.1038/nmat1726
35. **Franssen, G., Grzanka, S., Czernecki, R., Suski, T., Marona, L., Riemann, T., Christen, J., Teisseyre, H., Valvin, P., Lefebvre, P., Perlin, P., Leszczynski, M., Grzegory, I.** Efficient Radiative Recombination and Potential Profile Fluctuations in Low-dislocation InGaN/GaN Multiple Quantum Wells on Bulk GaN Substrates *Journal of Applied Physics* 97 2005: p. 103507. http://dx.doi.org/10.1063/1.1897066
36. **Graham, D. M., Soltani-Vala, A., Dawson, P., Godfrey, M. J., Smeeton, T. M., Bernard, J. S., Kappers, M. J., Humphreys, C. J.** Optical and Microstructural Studies of InGaN/GaN Single-Quantum-Well Structures *Journal of Applied Physics* 97 2005: p. 103508. http://dx.doi.org/10.1063/1.1897070
37. **Gotoh, H., Akasaka, T., Tawara, T., Kobayashi, Y., Makimoto, T., Nakano, H.** Detecting Spatially Localized Excitons in InGaN Quantum Well Structures with a Micro-photoluminescence Technique *Solid State Community* 138 2006: pp. 590 – 593.
38. **Galtrey, M. J., Oliver, R. A., Kappers, M. J., Humphreys, C. J., Clifton, P. H., Larson, D., Saxey, D. W., Cerezo A.** Three-dimensional Atom Probe Analysis of Green- and Blue-emitting $In_xGa_{1-x}N$/GaN Multiple Quantum Well Structures *Journal of Applied Physics* 104 2008: p. 013524. http://dx.doi.org/10.1063/1.2938081
39. **Varshni, Y. P.** Band-to-band Radiative Recombination in Groups IV, VI, and III-V Semiconductors *Physica Status Solidi* 19 1967: pp. 459 – 514. http://dx.doi.org/10.1002/pssb.19670190202
40. **Vina, L., Logothetidis, S., Cardona, M.** Temperature Dependence of the Dielectric Function of Germanium *Physical Review B* 30 1984: p. 1979.
41. **Ivchenko, E. L., Reznitsky, A. N.** Hopping and Low-temperature Photoluminescence in Solid Solutions and Amorphous Semiconductors *Philosophical Magazine B* 65 1992: pp. 733 – 737.
42. **Monroe, D.** Hopping in Exponential Band Tails *Physics Review Letters* 54 1985: pp. 146 – 149. http://dx.doi.org/10.1103/PhysRevLett.54.146
43. **Zimmermann, R., Runge, E.** Excitons in Narrow Quantum Wells: Disorder Localization and Luminescence Kinetics *Physica Status Solidi A* 164 1997: pp. 511 – 516.
44. **Kazlauskas, K., Tamulaitis, G., Pobedinskas, P., Žukauskas, A., Springis, M., Huang, C.-F., Cheng, Y.-C. Yang, C. C.** Exciton Hopping in $In_xGa_{1-x}N$ Multiple Quantum Wells *Physics Review B* 71 2005: p. 085306. http://dx.doi.org/10.1103/PhysRevB.71.085306
45. **Chichibu, S., Wada, K., Nakamura, S.** Spatially Resolved Cathodoluminescence Spectra of InGaN Quantum Wells *Applied Physics Letters* 71 1997: p. 2346. http://dx.doi.org/10.1063/1.120025
46. **Humphreys, C. J.** Does In Form In-rich Clusters in InGaN Quantum Wells *Philosophical Magazine* 87 2007: p. 1971. http://dx.doi.org/10.1080/14786430701342172
47. **Bertram, F., Srinivasan, S., Geng, L., Ponce, F. A., Riemann, T., Christen, J., Tanaka, S., Omiya, H., Nakagawa, Y.** Spatial Variation of Luminescence of InGaN Alloys Measured by Highly-Spatially-Resolved Scanning Catholuminescence *Physica Status Solidi B* 228 2001: pp. 35 – 39. http://dx.doi.org/10.1002/1521-3951(200111)228:1<35::AID-PSSB35>3.0.CO;2-1
48. **Cherns, D., Henley, S. J., Ponce, F. A.** Edge and Screw Dislocations as Nonradiative Centers in InGaN/GaN Quantum Well Luminescence *Applied Physics Letters* 78 2001: p. 2691. http://dx.doi.org/10.1063/1.1369610
49. **Brooksby, J. C., Mei, J., Ponce, F. A.** Correlation of Spectral Luminescence with Threading Dislocations in Green-light-emitting InGaN Quantum Wells *Applied Physics Letters* 90 2007: p. 231901. http://dx.doi.org/10.1063/1.2746062
50. **Oh, E., Park, H., Sone, C., Nam, O., Park, Y., Kim, T.** Micro-photoluminescence Study of $In_xGa_{1-x}N$/GaN Quantum Wells *Solid State Community* 113 2000: pp. 461 – 464.
51. **Gotoh, H., Akasaka, T., Tawara, T., Kobayashi, Y., Makimoto, T., Nakano, H.** Detecting Spatially Localized Excitons in InGaN Quantum Well Structures with a Micro-photoluminescence Technique *Solid State Community* 138 2006: pp. 590 – 593.
52. **Ko, T. S., Lu, T. C., Wang, T. C., Chen, J. R., Gao, R. C., Lo, M. H., Kuo, H. C., Wang, S. C., Shen, J. L.** Optical Study of a-plane InGaN/GaN Multiple Quantum Wells with Different Well Widths Grown by Metal-organic Chemical Vapor Deposition *Journal of Applied Physics* 104 2008: p. 093106.
53. **O'Donnell, K. P., Cowan, C. T., Pereira, S., Bangura, A., Young, C., White, M. E., Tobin, M. J.** Spectroscopic Imaging of InGaN Epilayers *Physica Status Solidi B* 216 1999: pp. 157 – 161. http://dx.doi.org/10.1002/(SICI)1521-3951(199911)216:1<157::AID-PSSB157>3.0.CO;2-K
54. **Vierheilig, C., Braun, H., Schwarz, U. T., Wegscheider, W., Baur, E., Strauß, U., Harle, V.** Lateral Diffusion of Photogenerated Carriers in InGaN/GaN Heterostructures Observed by PL Measurements *Physica Status Solidi C* 4 2007: pp. 2362 – 2365. http://dx.doi.org/10.1002/pssc.200674771
55. **Okamoto, K., Kaneta, A., Kawakami, Y. Fujita, S., Choi, J., Terazima, M., Mukai, T.** Confocal Microphotoluminescence of InGaN-based Light-emitting Diodes *Journal of Applied Physics* 98 2005: p. 064503. http://dx.doi.org/10.1063/1.2037869
56. **Hitzel, F., Hangleiter, A., Bader, S., Lugauer, H.-J., Härle, V.** Correlation of Defects and Local Bandgap Variations in GaInN/GaN/AlGaN LEDs *Physica Status Solidi B* 228 2001: pp. 407 – 410. http://dx.doi.org/10.1002/1521-3951(200111)228:2<407::AID-PSSB407>3.0.CO;2-Q

57. **Kaneta, A., Okamoto, K., Kawakami, Y., Fujita, S., Marutsuki, G., Narukawa, Y., Mukai, T.** Spatial and Temporal Luminescence Dynamics in an InxGa1-xN Single Quantum Well Probed by Near-field Optical Microscopy Luminescence *Applied Physics Letters* 81 2002: pp. 4353 – 4355.

58. **Okamoto, K., Kaneta, A., Kawakami, Y., Fujita, S., Choi, J., Terazima, M., Mukai, T.** Confocal Microphotoluminescence of InGaN-based Light-emitting Diodes *Journal of Applied Physics* 98 2005: p. 064503. http://dx.doi.org/10.1063/1.2037869

59. **Kaneta, A., Funato, M., Kawakami, Y.** Nanoscopic Recombination Processes in InGaN/GaN Quantum Wells Emitting Violet, Blue, and Green Spectra *Physics Review B* 78 2008: p. 125317.

60. **Narayan, J., Wang, H., Ye, J., Hon, S.-J., Fox, K., Chen, J. C., Choi, H. K., Fan, J. C. C.** Effect of Thickness Variation in High-efficiency InGaN/GaN Light-emitting Diodes *Applied Physics Letters* 81 2002: p. 841. http://dx.doi.org/10.1063/1.1496145

61. **Kwon, S.-Y., Kim, H. J., Yoon, E., Jang, Y., Yee, K.-J., Lee, D., Park, S.-H., Park, D.-Y., Cheong, H., Rol, F., Dang, L. S.** Optical and Microstructural Studies of Atomically Flat Ultrathin In-rich InGaN/GaN Multiple Quantum Wells *Journal of Applied Physics* 103 2008: p. 063509. http://dx.doi.org/10.1063/1.2874494

62. **Sonderegger, S., Feltin, E., Merano, M., Crottini, A., Carlin, J. F., Sachot, R., Deveaud, B., Grandjean, N., Ganiere, J. D.** High Spatial Resolution Picosecond Cathodoluminescence of InGaN Quantum Wells *Applied Physics Letters* 89 2006: p. 232109. http://dx.doi.org/10.1063/1.2397562

63. **Dobrovolskas, D., Mickevičius, J., Kuokštis, E., Tamulaitis, G., Shur, M., Shatalov, M., Yang, J., Gaska, R.** Confocal Spectroscopy of InGaN LED Structures *Journal of Physics D: Applied Physics* 44 2011: p. 135104. http://dx.doi.org/10.1088/0022-3727/44/13/135104

64. **Hangleiter, A., Hitzel, F., Netzel, C., Fuhrmann, D., Rossow, U., Ade, G., Hinze, P.** Suppression of Nonradiative Recombination by V-shaped Pits in GaInN/GaN Quantum Wells Produces a Large Increase in the Light Emission Efficiency *Physics Review Letters* 95 2005: p. 127402.

65. **Yong-Hoon, Cho, Y-H., Gainer, G. H., Lam, J. B., Song, J. J., Yang, W., Jhe, W.** Dynamics of Anomalous Optical Transitions in $Al_xGa_{1-x}N$ Alloys *Physics Review B* 61 2000: pp. 7203 – 7206.

66. **Kim, H. S., Mair, R. A., Li, J., Lin, J. Y., Jiang, H. X.** Time-resolved Photoluminescence Studies of $Al_xGa_{1-x}N$ alloys *Applied Physics Letters* 76 2000: p. 1252. http://dx.doi.org/10.1063/1.126000

67. **Bell, A., Srinivasan, S., Plumlee, C., Omiya, H., Ponce, F. A., Christen, J., Tanaka, S., Fujioka, A., Nakagawa, Y.** Exciton Freeze-out and Thermally Activated Relaxation at Local Potential Fluctuations in Thick $Al_xGa_{1-x}N$ layers *Journal of Applied Physics* 95 2004: p. 4670. http://dx.doi.org/10.1063/1.1689736

68. **Kazlauskas, K., Žukauskas, A., Tamulaitis, G., Mickevičius, J., Shur, M. S., Fared, R. S. Q., Zhang, J. P., Gaska, R.** Exciton Hopping and Nonradiative Decay in AlGaN Epilayers *Applied Physics Letters* 87 2005: p. 172102. http://dx.doi.org/10.1063/1.2112169

69. **Collins, C. J., Sampath, A. V., Garrett, G. A., Sarney, W. L., Shen, H., Wraback, M., Nikiforov, A. Y., Cargill, G. S. III, Dierolf, V.** Enhanced Room-temperature Luminescence Efficiency through Carrier Localization in $Al_xGa_{1-x}N$ Alloys *Applied Physics Letters* 86 2005: p. 031916. http://dx.doi.org/10.1063/1.1856702

70. **Murotani, H., Saito, T., Kato, N., Yamada, Y., Taguchi, T., Ishibashi, A., Kawaguchi, Y., Yokogawa, T.** Localization - Induced Inhomogeneous Screening of Internal Electric Fields in AlGaN-based Quantum *Applied Physics Letters* 91 2007: p. 231910. http://dx.doi.org/10.1063/1.2817749

71. **Pinos, A., Liuolia, V., Marcinkevicius, S., Yang, J, Gaska, R., Shur, M. S.** Localization Potentials in AlGaN Epitaxial Films Studied by Scanning Near-field Optical Spectroscopy *Journal of Applied Physics* 109 2011: p. 113516.